

RESEARCH

Open Access



Neuroprotective, and memory enhancement effects of *Salvia aristata* and its phenolic constituents: an in vitro, and in vivo study

Farid Dabaghian¹, Mohammad-Reza Delnavazi¹, Roshanak Hariri², Tahmineh Akbarzadeh², Zahra Tayarani-Najaran³, Mohammad Reza Shams Ardekani¹, Mohammad Sharifzadeh⁴ and Mahnaz Khanavi^{1*}

Abstract

Background Alzheimer's disease (AD) is a progressive neurodegenerative disorder characterized by cholinergic dysfunction, neuroinflammation, oxidative stress, and memory impairment. The *Salvia* genus has been used since ancient times for its anti-inflammatory and neuroprotective properties. In this study, we aimed to investigate the effects of *Salvia aristata* hydroalcoholic extract (SAHE) and dichloromethane extract (SADE) on various aspects of memory and AD.

Methods Column chromatography was utilized in the phytochemical analysis to isolate and purify bioactive compounds. The structures of the isolated compounds were determined through spectroscopic techniques, including 1D and 2D NMR, along with IR, UV, and HRESIMS for the new compound. Cholinesterase inhibitory activity was assessed using a modified Ellman's method. Additionally, the antioxidant activity and metal chelation capacity of SAHE and SADE were evaluated using the DPPH assay and spectroscopic methods, respectively. Moreover, the neuroprotective effects in PC12 cells were investigated using the AlamarBlue assay, and the ability to mitigate scopolamine-induced memory impairment in rats was assessed using the Morris water maze (MWM) test.

Results In this study, we isolated and structurally elucidated an undescribed compound, namely salvinarin (**2**), as well as four known compounds including linariin (**1**), pectolinarin (**3**), scutellarein 4'-O-methyl-7-O-rutinoside (**4**), and 5-O-coumaroylquinic acid (**5**) from SAHE for the first time. In vitro analyses revealed that SAHE, SADE, and linariin exhibited significant neuroprotective effects against H₂O₂-induced cytotoxicity in PC12 cells. Notably, SAHE demonstrated potent acetylcholinesterase (AChE) inhibition (IC₅₀ = 322.83 ± 1.11 μg/mL), significant antioxidant activity (IC₅₀ = 99.16 ± 1.24 μg/mL), and strong metal chelating capacity toward Cu²⁺, Zn²⁺, and Fe²⁺. Moreover, oral administration of SAHE (400 mg/kg/day) significantly ameliorated memory impairment induced by scopolamine in a rat model. This improvement was evident in parameters such as traveled distance ($p < 0.001$), escape latency ($p < 0.001$), and time spent in the target quadrant ($p < 0.01$) in the Morris water maze test.

*Correspondence:

Mahnaz Khanavi

khanavim@tums.ac.ir; mahnazkhanavi@yahoo.ca

Full list of author information is available at the end of the article

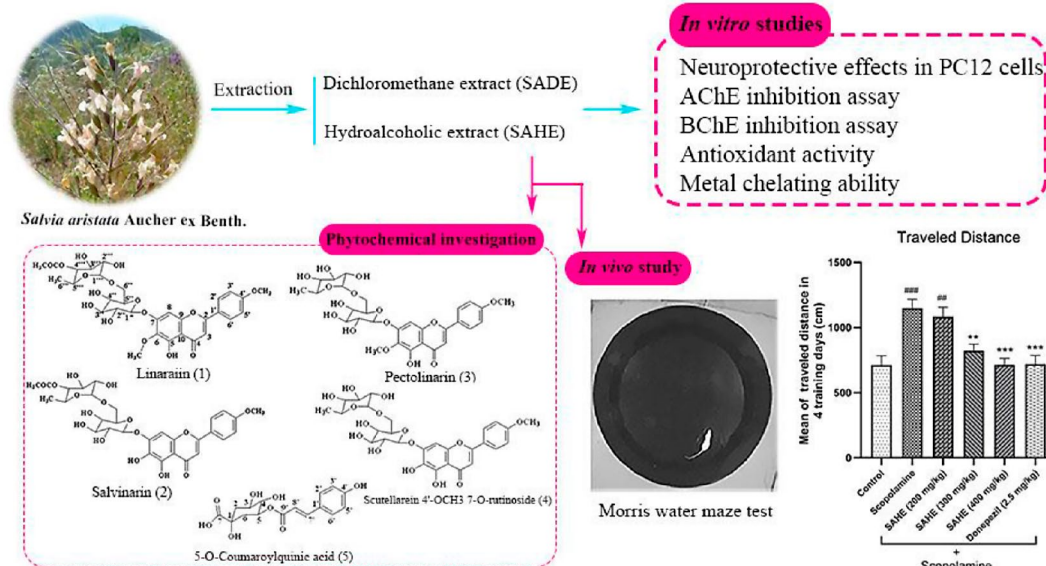


© The Author(s) 2025. **Open Access** This article is licensed under a Creative Commons Attribution-NonCommercial-NoDerivatives 4.0 International License, which permits any non-commercial use, sharing, distribution and reproduction in any medium or format, as long as you give appropriate credit to the original author(s) and the source, provide a link to the Creative Commons licence, and indicate if you modified the licensed material. You do not have permission under this licence to share adapted material derived from this article or parts of it. The images or other third party material in this article are included in the article's Creative Commons licence, unless indicated otherwise in a credit line to the material. If material is not included in the article's Creative Commons licence and your intended use is not permitted by statutory regulation or exceeds the permitted use, you will need to obtain permission directly from the copyright holder. To view a copy of this licence, visit <http://creativecommons.org/licenses/by-nc-nd/4.0/>.

Conclusions Considering all findings, including significant neuroprotective, antioxidant, and metal-chelating properties, alongside notable efficacy in enhancing memory in rat models, *S. aristata* could be a potential candidate for memory improvement.

Keywords *Salvia aristata*, Lamiaceae, Flavonoid, Polyphenols, Alzheimer's disease, Memory, Neuroprotection, Oxidative stress

Graphical Abstract



Background

Alzheimer's disease (AD) is a progressive amnesic disorder characterized by cognitive decline, memory impairment, and various behavioral and neuropsychiatric changes [1]. While the precise mechanisms underlying AD remain incompletely understood, key pathological features include cholinergic dysfunction, oxidative stress, neuroinflammation, and the accumulation of amyloid-beta ($A\beta$) plaques [2]. Among these, cholinergic dysfunction -particularly in the cortical and hippocampal regions- plays a critical role in the cognitive deficits observed in AD. On the other hand, changes in the metabolism of the amyloid precursor protein and the phosphorylation of tau are associated with cholinergic system abnormalities, which can lead to neuroinflammation and neuronal death [3]. Cholinergic neurons are crucial for learning and memory, and their degeneration has been linked to deficits in neurogenesis, decreased levels of choline acetyltransferase, and impaired memory functions [4]. Consequently, one of the primary clinical approaches to address AD involves the restoration of the cholinergic system in the human body.

Along with cholinergic imbalance, oxidative stress, and reactive oxygen species (ROS) accumulation, other factors such as dyshomeostasis of bio-metal ions (Cu^{2+} , Fe^{2+} , and Zn^{2+}) at the cellular and organismal levels,

glymphatic system malfunction, and tau protein hyperphosphorylation and neurofibrillary tangle formation are linked to the pathophysiology of AD [5]. Given the multifactorial nature of AD, a more effective treatment approach would involve compounds that target multiple pathological mechanisms simultaneously. In this regard, medicinal plants, and their derived natural compounds, have gained significant attention for their ability to modulate various molecular targets. Moreover, the use of medicinal plants for the prevention and treatment of various diseases is of great interest among people [6], which further underscores their use in managing conditions such as AD. These compounds often exhibit antioxidant, anti-inflammatory, and neuroprotective properties, making them promising candidates for AD management [7].

Recent studies have highlighted the neuroprotective potential of extracts and their bioactive compounds in AD therapy. For instance, the aqueous extract of *Cyperus esculentus* L. has been shown to mitigate oxidative stress and improve memory function in scopolamine-induced mice by significantly reducing brain levels of AChE, malondialdehyde, and nitrite [8]. Additionally, polyphenols have emerged as promising multitargeted agents for managing neurodegenerative diseases, including AD [9]. These compounds exert neuroprotective effects through multiple mechanisms, including

antioxidant activity, modulation of neuroinflammation, inhibition of A β aggregation, and enhancement of cholinergic neurotransmission [10, 11]. Notably, curcumin and resveratrol have demonstrated significant therapeutic potential against AD in several studies [12, 13]. Furthermore, synthetic curcumin analogs have exhibited AChE inhibitory effects, with IC₅₀ values ranging from 112.52 to 5839.96 nM. Among these, a synthetic analog containing a chlorine substituent on the aromatic rings displayed the highest activity and significantly improved cognitive performance in mice. At oral doses of 7.5 and 15 mg/kg/day, this analog effectively reversed scopolamine-induced amnesia in behavioral tests, including the elevated plus maze, Y-maze, and novel object recognition test [14].

Among the numerous medicinal plants investigated, *Salvia* species have garnered attention due to their traditional use in improving memory and cognitive function. In the 16th century, the herbalist John Gerard described it as beneficial for brain function, highlighting its potential to enhance memory and stimulate neural activity [15]. Moreover, recent investigations have demonstrated the efficacy of various *Salvia* species in addressing memory and AD. For instance, Sezer Şenol et al. identified that *Salvia fruticosa* Mill. extract inhibited AChE activity by 51.07% at 100 μ g/mL [16]. Similarly, another study reported that the extract of *Salvia staminea* Montbret & Aucher ex Benth. exhibited notable cholinesterase (ChE) inhibitory activity, with 55.17% inhibition of AChE and 79.75% inhibition of butyrylcholinesterase (BChE) at 200 μ g/mL [17]. Additionally, several cellular studies have substantiated the neuroprotective effects of *Salvia* species. For example, Ververis et al. demonstrated that pre-treating SH-SY5Y cells with 20 μ g/mL of petroleum ether extract of *S. fruticosa* significantly reduced the toxicity induced by A β _{25–35} compared to cells exposed solely to A β _{25–35} [18].

In addition to in vitro experiments, some *Salvia* species have been studied for their effectiveness in animal models of memory impairment, emphasizing the necessity of both approaches to obtain reliable conclusions about their memory-enhancing properties. For instance, *Salvia officinalis* L. exhibited moderate AChE inhibitory activity, with an IC₅₀ value of 268.45 μ g/mL, while galantamine, used as a positive control, had an IC₅₀ of 0.12 μ g/mL [19]. However, in animal studies, the oral administration of *S. officinalis* extract significantly alleviated scopolamine-induced memory impairment in mice. The group receiving 400 mg/kg of the extract demonstrated a substantial reduction in escape latency time (21.37 \pm 1.38 s) compared to the scopolamine-treated group (102.34 \pm 1.34 s), suggesting a notable neuroprotective effect [20]. Similarly, Ayoub et al. reported that oral administration of *S. officinalis* and *Salvia microphylla* Kunth extracts improved cognitive performance in a

scopolamine-induced rat model, with enhancements of 1.62 to 2.01 fold in probe trial performance compared to the scopolamine-treated group [21]. Moreover, although the ethanolic extract of *Salvia multiorrhiza* Bunge demonstrated relatively weak in vitro AChE inhibition (27% at 2 mg/mL) [22], its effects on memory enhancement were significant in a scopolamine-induced rat model of memory impairment [23]. Consequently, it can be concluded that both in vitro assessments (such as ChE inhibitory effects, neuroprotective, and antioxidant activities) and animal studies should be considered to provide more conclusive evidence of the memory-enhancing effects of *Salvia* species.

While various *Salvia* species have shown promising therapeutic potential, the effects of *Salvia aristata* Aucher ex Benth. on memory and AD remain largely unexplored. This perennial herb, endemic to Iran and eastern Turkey [24], has not yet been thoroughly investigated for its bioactive compounds, with existing research limited to its essential oil composition [25]. Additionally, *S. aristata*, commonly known as “*Maryam goli-e-sikhakdar*” in Iran, has exhibited neuroprotective properties by attenuating H₂O₂-induced oxidative stress in SH-SY5Y neuroblastoma cells. These protective effects are mediated through the downregulation of apoptosis-related genes such as Caspase 3, Bax, and Caspase 9 and the upregulation of the anti-apoptotic gene Bcl-2. Furthermore, *S. aristata* preserves mitochondrial membrane integrity, prevents the release of cytochrome *c* into the cytosol, and inhibits apoptotic cell death. These findings suggest that *S. aristata* exerts its neuroprotective effects through a series of interconnected mechanisms [26]. However, its bioactive compounds and therapeutic potential in AD models (in vitro, and in vivo have yet to be fully characterized. Therefore, this study aims to explore the therapeutic potential of *S. aristata* in AD by pursuing the following objectives: (1) evaluating the anti-AChE and anti-BChE activities of its extracts and fractions; (2) isolating and elucidating structure of bioactive compounds; (3) assessing its antioxidant and metal chelating activity, two factors involved in memory, and AD pathophysiology; and (4) studying the neuroprotective effects of *S. aristata* extracts, and major isolated compound against H₂O₂-induced neurotoxicity in PC12 cells, as well as its inhibitory potential on cognitive and memory impairments in a scopolamine-induced rat model of AD.

Materials and methods

General experimental procedures

The NMR spectra were obtained at 25 °C using an AVANCE III spectrometer (Bruker BioSpin) set to 300.81 MHz for ¹H-NMR and 75.65 MHz for ¹³C-NMR, 2D HSQC, and HMBC spectra. The results were given in

ppm units relative to TMS. HRESI-MS data was obtained using a Waters LCT Premier mass spectrometer. The UV spectroscopic data were obtained using a UV-1800 spectrophotometer (Shimadzu) with a scanning range of 250 to 550 nm. The optical rotation was measured with sodium D line (590 nm) using a Perkin-Elmer 241 polarimeter instrument (Perkin-Elmer). Infrared spectra (IR) were analyzed by using a Nicolet is10 spectrophotometer equipped with an attenuated reflectance (ATR) containing a diamond crystal (Thermo Scientific) in the 400–4000 cm^{-1} scan range. Column chromatography (CC) was conducted using silica gel with mesh sizes of 70–230 and 230–400 (Merck) and Sephadex LH-20 (Pharmacia). Thin-layer chromatography (TLC) plates measuring 20 × 20 cm, pre-coated with silica gel F₂₅₄ were acquired from Merck. Spots on TLC plates were observed under UV illumination (254 and 365 nm) (CAMAG). Also, anisaldehyde-sulfuric acid was applied, followed by heating at 120 °C. The absorbance intensity of 96-well plates during the cell viability test was assessed using a microplate reader (Synergy H4 Hybrid Multi-Mode, BioTek).

Chemicals and reagents

AChE (Type V-S, lyophilized powder, E.C. 3.1.1.7, 1000 unit, from electric eel), BChE (E.C. 3.1.1.8, from equine serum), butyrylthiocholine iodide (BTCI), acetylthiocholine iodide (ATCI), *p*-nitrophenyl α -D-glucopyranoside (*p*-NPG), 5,5'-dithio-bis-(2-nitrobenzoic acid) (DTNB), scopolamine hydrobromide (purity ~ 95%), donepezil hydrochloride (purity > 98%), AlamarBlue, and RPMI were purchased from Sigma-Aldrich. Potassium

dihydrogen phosphate, dipotassium hydrogen phosphate, sodium hydrogen carbonate, and potassium hydroxide were purchased from Fluka. The extraction and CC solvents were of technical grade and were redistilled before use. Also, we purchased penicillin-streptomycin (Pen-Strep) and fetal bovine serum (FBS) from Gibco.

Plant material

The aerial parts of *S. aristata* were collected in May 2021 from their natural habitat in Fereydan, located in the western region of Isfahan province, Iran (Fig. 1). The plants were harvested during the flowering stage under mild spring conditions with moderate humidity. Identification of the plant was confirmed by botanist Mr. M.T. Feyzi (Agriculture & Natural Resources Research Center of Isfahan, Iran). A voucher specimen (7082-TEH) of this plant was deposited at the herbarium of the School of Pharmacy, Tehran University of Medical Sciences, Tehran, Iran. Experimental research and field studies on plants, including the collection of plant material, comply with relevant institutional, national, and international guidelines and legislation.

Extraction

The aerial parts of *S. aristata* were air-dried in the shade at room temperature for one week. After that, it was converted into crushed parts using the grinder. To obtain *S. aristata* dichloromethane extract (SADE), the ground powder (1 kg) was macerated for 3 × 72 h in 5 L of dichloromethane (the solvent was replaced every 72 h). The plant residue was then used to yield *S. aristata*



Fig. 1 *Salvia aristata* Aucher ex Benth. in its natural habitat

hydroalcoholic (70% MeOH) extract (SAHE) as directed for SADE. The obtained extracts underwent filtration using filter paper and concentration in a rotary evaporator under reduced pressure at below 40 °C. The SADE was obtained as a semi-solid, sticky residue due to the presence of non-polar compounds, whereas SAHE was obtained in powdered form after drying. At the end, they were kept at -20 °C until further analysis.

Isolation and characterization

The chromatographic process was performed based on the AChE inhibitory activity of the extracts, utilizing 80 g of SAHE for CC (9 × 15 cm) on silica gel (70–230 mesh). The sample was eluted using a gradient of CHCl₃:MeOH (90:10 → 0:100, v/v) to afford 22 individual fractions. Based on the TLC results (detection of bands using UV (254 and 365 nm) and visualization by anisaldehyde-sulfuric acid spray), the fractions displaying similar spots were mixed to give five distinct fractions (I–V). Compound **1** (12 g) was isolated from fraction I using the recrystallization method with CHCl₃. Fraction II was subjected to normal phase CC (230–400 mesh, 3 × 40 cm) with a gradient solvent system of CH₂Cl₂:MeOH (100:0 → 75:25, v/v) to afford 33 subfractions (B₁– B₃₃). After that, a mixture of B₇ and B₈ was applied on the Sephadex LH-20 column with MeOH as a mobile phase to purify compound **2** (17.1 mg).

Fraction IV was chromatographed on another normal phase CC (230–400 mesh, 4.5 × 45 cm) and eluted with a gradient mixture of CH₂Cl₂:MeOH (100:0 → 60:40, v/v) to give 60 subfractions (C₁– C₆₀). Compound **3** (16.7 mg) was purified from subfraction C₁ by recrystallization with CHCl₃. Loading of C₃₄ and the mixture of C₄₃– C₄₇ onto different Sephadex LH-20 and eluting with MeOH:H₂O (80:20, v/v) led to the isolation of compounds **4** (25 mg) and **5** (32.4 mg), respectively.

In vitro cholinesterase inhibitory activity

AChE, and BChE inhibitory assays were applied on SAHE and SADE, as well as various obtained fractions by CC, and isolated compounds using the modified Ellman's method, precisely following the procedures outlined previously [27]. To achieve the desired enzyme inhibitory activity, we prepared initial solutions of the extracts and fractions at a concentration of 10 mg/mL and pure compounds at 1 mg/mL using DMSO. These solutions were further diluted with a mixture of DMSO and methanol to yield four distinct final concentrations for the extracts, fractions (63.5, 125, 250, 500 μg/mL), as well as for the pure compounds (1, 10, 20, 40 μg/mL) while preserving a final ratio of 50/50 (DMSO/ MeOH). In each well, there were 25 μL of the above-mentioned prepared sample, along with 50 μL of potassium phosphate buffer (KH₂PO₄/ K₂HPO₄, 0.1 M, pH 8) and AChE (25 μL)

at a final concentration of 0.22 units/mL in the buffer. A pre-incubation of 15 min at room temperature was carried out before adding 125 μL of DTNB (3 mM in buffer). Following that, 25 μL of the substrate (ATCI, 3 mM in water) was introduced into the mixture, and changes in absorbance were spectrometrically assessed at 405 nm. To consider the non-enzymatic reaction, a blank, consisting of all components except the enzyme, was employed simultaneously. Furthermore, a negative control without an inhibitor was included, and donepezil served as a positive control under the same conditions. Finally, the IC₅₀ values were calculated graphically through the analysis of log concentration versus inhibition (%) curves for samples that showed an inhibition greater than 50% at the highest concentration. Every experiment was done in triplicate. The same procedure was utilized to assess BChE inhibitory effects with BTCl as the substrate.

Antioxidant activity by DPPH method

One of the most widely used techniques for determining the antioxidant properties of medicinal plants involves the utilization of the 1, 1-diphenyl-2-picrylhydrazyl (DPPH) radical [28]. Briefly, this experiment was carried out using several concentrations of SAHE and SADE (7.81, 15.62, 31.25, 62.5, 125, 250, 500, and 1000 μg/mL), which were prepared in MeOH. Five mL of DPPH methanolic solution (0.08 mg/mL) were added to the aliquots of each concentration of the extract (5 mL). The final mixture was thoroughly shaken and then allowed to incubate in a dark place at room temperature for 30 min. Subsequently, the absorbance at 517 nm was determined using a UV spectrophotometer. In the same method, quercetin was used as the positive control. Each experiment was conducted three times. The following formula was used to calculate the percentage of scavenging activity:

$$\text{Scavenging activity (\%)} = \left[\frac{(\text{Abs}_{\text{blank}} - \text{Abs}_{\text{sample}})}{(\text{Abs}_{\text{blank}})} \right] \times 100$$

Here, the Abs_{sample} represents the absorbance of the extracts, and the Abs_{blank} is the absorbance of the blank (containing DPPH in MeOH at a 1:1 ratio). The IC₅₀ values (μg/mL) were utilized to represent the DPPH radical scavenging activity of the extracts, which was calculated using a linear regression plot of extract concentrations versus inhibition percentages.

Metal ion chelating ability

For this experiment, all solutions, including extracts and metal ions, were prepared in methanol and the test was carried out based on Rastegari et al. [29]. Cu²⁺, Fe²⁺, and Zn²⁺ ion solutions were prepared using CuCl₂·2H₂O, FeSO₄·7H₂O, and ZnCl₂, respectively. To assess the

bio-metal chelating capability, the absorbance of the methanolic solutions of the extracts (31.25 and 250 $\mu\text{g}/\text{ml}$ for SAHE and SADE, respectively) was initially measured in the wavelength range of 260–550 nm. After that, an equal volume of extract solution and targeted metal ions (final concentration of 20 μM) were mixed and allowed to react at room temperature for 30 min. Finally, the absorbance of the mixture in a 1 cm quartz cuvette was measured in the spectral range from 260 to 550 nm and compared with the absorbance acquired from the extract alone.

Cell culture

PC12 cells, derived from rat pheochromocytoma, were obtained from the National Cell Bank of Iran, Pasteur Institute. Cells were cultured in RPMI-1640 medium supplemented with 1% Pen-Strep and 10% v/v FBS in a controlled setting at 37 °C with a humidified atmosphere containing 5% CO_2 . The RPMI-1640 medium was replaced every 48 h. Finally, the seeding of cells was carried out with a density of 5×10^3 cells in each well in a 96-well plate and then incubated for 24 h. SAHE, SADE, and compound **1** (linariin) as a major bioactive isolated compound were selected for this assay.

Cell viability analysis and neuroprotectivity assay

At first, the cytotoxicity of the samples was assessed based on the AlamarBlue test as described by Hadipour et al. [30]. In this assay, resazurin serves as an indicator of the reducing power of viable cells and is used to evaluate cell viability. Following a 24 h incubation of the seeded cells in 96-well plates, the cells were subjected to treatment with the extracts at concentrations of 2.5, 5, 10, and 20 $\mu\text{g}/\text{mL}$, and compound **1** (linariin) at 12.5, 25, 50, and 100 μM for 24 h. Finally, AlamarBlue (10% v/v) was introduced to each well, and subsequently, the cells were incubated for 4–6 h at 37 °C. The absorbance at 600 nm was determined using a microplate reader. This experiment was performed in triplicate.

To investigate the neuroprotective properties of the samples against H_2O_2 -induced apoptosis in PC12 cells, the cells were seeded at a density of 5×10^3 cells/well in 96-well plates and incubated for 24 h. They were then pretreated with the extracts at concentrations of 2.5, 5, 10, and 20 $\mu\text{g}/\text{mL}$, and compound **1** (linariin) at 12.5, 25, 50, and 100 μM for 24 h. Subsequently, the cells were exposed to 500 μM H_2O_2 for 24 h, following which the AlamarBlue test and analysis were conducted using the aforementioned procedure [30]. In addition, N-acetyl cysteine (NAC) was employed at a concentration of 5 mM as a positive control using the same methodology described earlier. This experiment was performed in triplicate.

Learning and memory evaluation by Morris water maze test

Animals

The experimental male albino Wistar rats (200–220 g) were obtained from the Faculty of Pharmacy, Tehran University of Medical Sciences, Tehran, Iran. The animals were housed in an animal facility with a 12-h light/dark cycle (lights on from 7:00 to 19:00) at a controlled temperature (25 ± 2 °C) and relative humidity ($60 \pm 10\%$). They were randomly divided into seven groups, with each group consisting of seven rats. Water and food were made available ad libitum. Animal treatment and maintenance were carried out in strict compliance with the “Institutional Guide for the Care and Use of Laboratory Animals” guidelines and were approved by the Tehran University of Medical Sciences Ethical Committee for the Care and Use of Laboratory Animals (approval ID: IR.TUMS.TIPS.REC.1398.153 at January 4th 2020).

Morris water maze test

The Morris water maze (MWM) test was utilized to evaluate spatial learning and memory as previously described [31]. The maze consisted of a black circular tank (60 cm in height and 136 cm in diameter) filled to 35 cm with warm water (25 ± 2 °C). Walls were covered with various shaped visual cues. The swimming pool was segregated into 4 equal quadrants, and a circular-shaped transparent platform with a diameter of 10 cm was submerged 1 cm below the water surface in the central area of the tank's northwest quadrant (target quadrant). The MWM test was conducted over four consecutive days for training and one day later for testing. The swimming trajectory of each rat, starting from the initial position to the platform, was tracked and pertinent data were documented utilizing a video camera-based Ethovision system (Noldus Information Technology, Wageningen, Netherlands). In each training day, the rats were subjected to four 90-second trials, during which they were placed in water within a randomly chosen quadrant of the pool. They were permitted to swim freely for a maximum duration of 90 s. If the rats did not locate the platform within this duration, the experimenter guided them to the platform and allowed them to remain there for 20 s. After that, quantitative data was presented in terms of traveled distance, escape latency, and swimming speed during the initial four days of training. On the fifth day, the rats were not treated, and a probe trial test (in which the platform was eliminated from the pool) was carried out to record time spent in the target quadrant (Q1). However, they received treatment for four days during the training period.

Treatments in animals

The SAHE was suspended in 5% ethanol in distilled water solution using a sonicator probe at approximately 40 °C,

while scopolamine and donepezil were dissolved in normal saline. Seven groups of rats ($n=7$ per group) were investigated in this study: (1) Control group was received normal saline (5 mL/kg/day, p.o.) 2 h prior to testing, (2) Scopolamine group was given scopolamine hydrobromide (4 mg/kg/day, i.p.) 30 min before the behavioral test, (3) Vehicle group was administered 5% ethanol in distilled water (5 mL/kg/day, p.o.) 2 h prior to test, (4) SAHE 200 mg group was administered SAHE (200 mg/kg/day, p.o.) and scopolamine (4 mg/kg/day, i.p.), 2 h and 30 min before test, respectively, (5) SAHE 300 mg group was received SAHE (300 mg/kg/day, p.o.) and scopolamine (4 mg/kg/day, i.p.), 2 h and 30 min before test, respectively, (6) SAHE 400 mg group was given SAHE (400 mg/kg/day, p.o.) and scopolamine (4 mg/kg/day, i.p.), 2 h and 30 min before test, respectively, and (7) Donepezil group was administered donepezil (2.5 mg/kg/day, p.o.) and scopolamine (4 mg/kg/day, i.p.), 2 h and 30 min before test, respectively. The selection of SAHE doses was based on previous studies of *Salvia* species, which reported similar dose ranges exhibiting neuroprotective effects in animal models of memory impairment without causing significant toxicity [21, 32]. One day after completing the MWM test, all animals were euthanized using a saturated CO₂ gas chamber. A certified veterinarian then confirmed death by verifying the absence of both heart-beat and pulse.

Statistical analysis

The results of the antioxidant activity test have been expressed according to three measurements using Excel software (version 16.0, Microsoft Corporation).

Moreover, the IC₅₀ values for the ChE inhibitory assay were obtained by extrapolating from the log inhibitor concentration vs. percent of inhibition curves using Excel software (version 16.0, Microsoft Corporation). This calculation was based on data points plotted using a non-linear logarithmic model. Furthermore, each experiment was performed in triplicate. In addition, the GraphPad Prism software (version 6.07, Graph Pad) was used to perform statistical analysis on the cell viability and animal study results. One-way analysis of variance (ANOVA) and then Tukey's post-hoc multiple comparison tests were used for the comparison of various samples in the cell viability analysis, as well as the test groups, first 4 days of trials (training days), and post-training probe trial test in animal study. Statistical significance was specified as $p < 0.05$.

Results

Isolation of compounds from the *S. aristata*

Successive column chromatography process on SAHE, alongside spectroscopic analysis, led to the isolation, and structural characterization of an unreported flavonoid (compound 2, namely salvinarin), and four known compounds (compounds 1, 3, 4, and 5) from this plant for the first time (Fig. 2). Identification of the known compounds relied on their 1D (¹H, ¹³C, and DEPT 135 experiments) and 2D NMR (HSQC, and HMBC experiments) spectra, and comparing acquired data to those reported in the literature. These compounds were recognized as linariin (4''-O-acetyl pectolarin) (1), pectolarin (scutellarein 6, 4'-di-OCH₃ 7-O-rutinoside) (3), scutellarein 4'-O-methyl-7-O-rutinoside (4), and

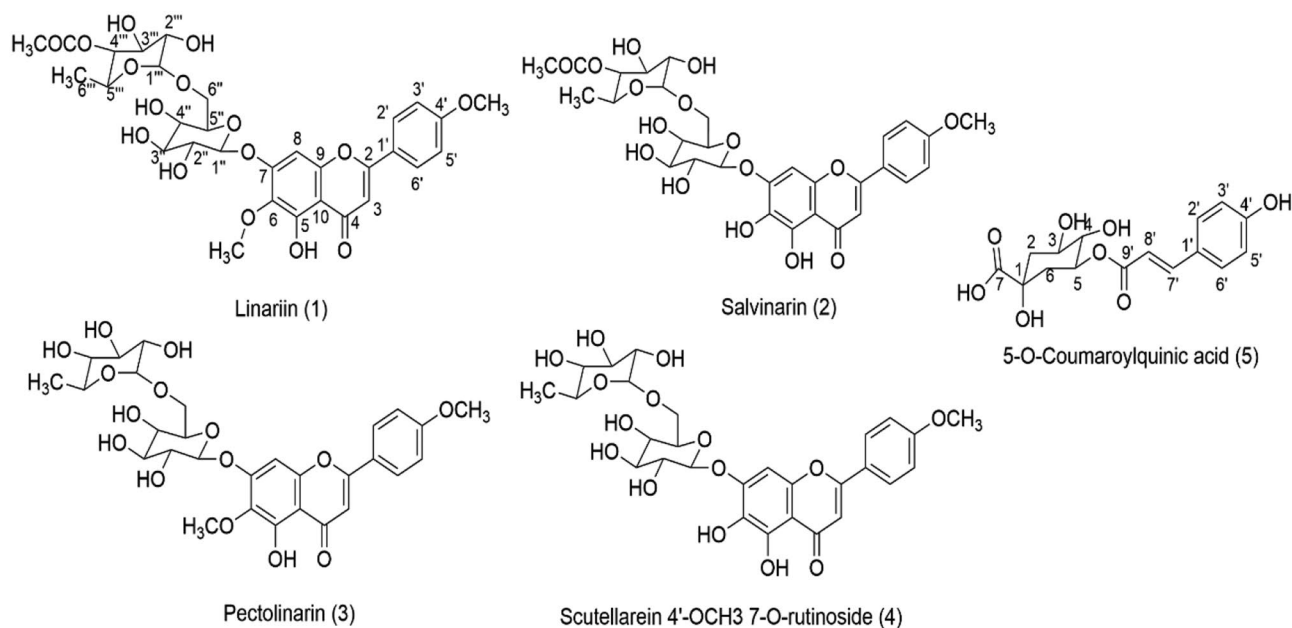


Fig. 2 The structure of isolated compounds (1–5) from the aerial parts of *S. aristata*

5-O-coumaroylquinic acid (5) [33–36]. The NMR spectra of the compounds are included in the supplementary file.

Linariin (4'''-O-acetyl pectolinarin) (1)

Pale yellow powder; MW = 664.61. ^1H NMR (DMSO- d_6): 12.97 (1H, s, 5-OH), 8.07 (2 H, d, J = 9.4 Hz, H-2' and H-6'), 7.15 (2 H, d, J = 9.4 Hz, H-3' and H-5'), 7.01 (1H, s, H-8), 6.96 (1H, s, H-3), 5.20 (1H, d, J = 7.1 Hz, Anomeric H-1''), 4.73 (1H, t, J = 9.6 Hz, H-4'''), 4.63 (1H, bs, Anomeric H-1'''), 3.88 (3 H, s, 4'-OMe), 3.80 (3 H, s, 6-OMe), 3.55–3.72 (3 H, m, H-2''', H-3''' and H-5''' of α -rhamnopyranose), 3.21–3.71 (6 H, m, H-2'' to H-6'' of β -glucopyranose), 1.99 (3 H, s, 4'''-OCOCH₃), 0.88 (3 H, d, J = 6.5 Hz, H-6'''). ^{13}C NMR (DMSO- d_6 , based on DEPT 135, HSQC, and HMBC experiments): 182.8 (C4), 170.4 (4'''-OCOCH₃), 164.4 (C2), 162.90 (C4'), 156.9 (C9), 153.0 (C7), 152.6 (C5), 133.2 (C6), 128.8 (C2' and C6') 123.1 (C1'), 115.1 (C3' and C5'), 106.3 (C10), 103.8 (C3), 100.6 (C1''), 100.4 (C1'''), 94.9 (C8), 76.9 (C3''), 75.8 (C5''), 74.3 (C4'''), 73.7 (C2''), 70.8 (C2'''), 69.7 (C4''), 68.7 (C3'''), 66.2 (C5'''), 66.0 (C6''), 60.7 (6-OMe), 56.0 (4'-OMe), 21.3 (4'''-OCOCH₃) 17.6 (C6''').

Salvinarin (2)

white-yellowish powder; R_f 0.38, silica gel 60 F254, CH_2Cl_2 :MeOH (80:20); UV (MeOH) λ_{max} (log ϵ) 286

(4.26) and 330 (4.33) nm; $[\alpha]_D^{25}$: -114.0° (c = 0.0016, MeOH); ATR-FTIR ν_{max} 3346.18, 2934.64, 1721.22, and 1659.96 cm^{-1} ; ^1H and ^{13}C NMR data (DMSO- d_6): 12.72 (1H, s, 5-OH), 8.04 (2 H, d, J = 8.7 Hz, H-2' and H-6'), 7.16 (2 H, d, J = 8.7 Hz, H-3' and H-5'), 6.95 (1H, s, H-8), 6.92 (1H, s, H-3), 5.07 (1H, d, J = 7.2 Hz, Anomeric H-1''), 4.75 (1H, t, J = 9.3 Hz, H-4'''), 4.66 (1H, bs, Anomeric H-1'''), 3.87 (3 H, s, 4'-OMe), 3.55–3.72 (3 H, m, H-2''', H-3''' and H-5''' of α -rhamnopyranose), 3.21–3.71 (6 H, m, H-2'' to H-6'' of β -glucopyranose), 1.99 (3 H, s, 4'''-OCOCH₃), 0.94 (3 H, d, J = 6.5 Hz, H-6'''). ^{13}C NMR (DMSO- d_6): 182.9 (C4), 170.4 (4'''-OCOCH₃), 164.2 (C2), 162.7 (C4'), 151.7 (C9), 149.5 (C7), 147.1 (C5), 130.9 (C6), 128.7 (C2' and C6') 123.3 (C1'), 115.2 (C3' and C5'), 106.4 (C10), 103.6 (C3), 101.3 (C1''), 100.5 (C1'''), 94.3

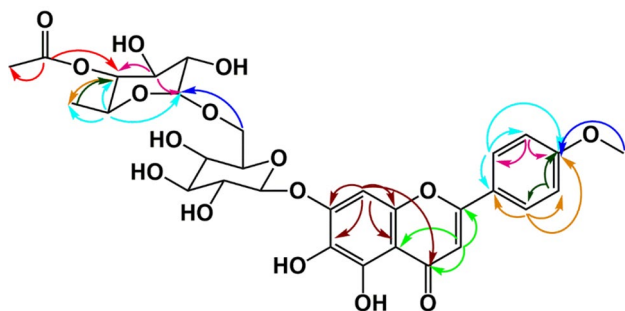


Fig. 3 The key HMBC correlations of compound 2 (salvinarin)

(C8), 76.0 (C3''), 74.3 (C5''), 74.3 (C4'''), 73.6 (C2''), 70.8 (C2'''), 69.9 (C4''), 68.7 (C3'''), 66.3 (C5'''), 66.2 (C6''), 56.0 (4'-OMe), 21.3 (4'''-OCOCH₃) 17.8 (C6'''). HRESI-MS (neg. ion mode) m/z 649.1791 $[\text{M}-\text{H}]^-$ (calculated for $\text{C}_{30}\text{H}_{33}\text{O}_{16}$, 649.1768).

This compound, identified as a new compound, was isolated as a white-yellowish powder. Its molecular formula, determined to be $\text{C}_{30}\text{H}_{34}\text{O}_{16}$ by HRESI-MS in negative ion mode, exhibited an ion peak at m/z 649.1791 $[\text{M}-\text{H}]^-$ (calculated for $\text{C}_{30}\text{H}_{33}\text{O}_{16}$, 649.1768). The ^1H , ^{13}C , HSQC, and HMBC NMR spectra of compound 2 revealed a structure similar to linariin; however, this molecule contains just one methoxy group. The ^{13}C , HSQC, and HMBC NMR spectra of compound 2 confirmed the presence of 27 carbon atoms and a single methoxy group. Based on the signals of ^{13}C NMR which resonating at δ_{C} 164.2 (C2), 103.6 (C3), and 182.9 (C4), as well as acquired data from DEPT-135 spectrum it could be perceived that this compound is belonged to a flavone subcategory. In addition, the presence of a C3 olefinic proton signal at δ_{H} 6.92 (1H, s, H-3) in the ^1H NMR spectrum confirmed this scaffold. The ^1H NMR spectrum (Fig. 6S) revealed the presence of an additional five aromatic protons. The proton resonances at δ_{H} 8.04 (2 H, d, H-2' and H-6'), and 7.16 (2 H, d, H-3' and H-5') exhibit coupling with a J value of 8.7 Hz, suggesting the existence of a B ring with *para*-substitution. Another aromatic proton appeared as a singlet at δ_{H} 6.95. The HMBC correlation revealed cross peaks of this aromatic proton with δ_{C} 106.4 (C10), 130.9 (C6), 149.5 (C7), and 151.7 (C9), indicating its attachment to C8, which resonates at δ_{C} 94.3.

Furthermore, in the HMBC spectrum, the hydrogens of the methoxy group (s, 3.87) showed a correlation with C4' (162.7), indicating that the methoxy was attached to C4', while H-4''' (t, 4.75) showed strong correlations with C6''' (17.8), C5''' (66.3), C3''' (68.7), and 4'''-OCOCH₃ (170.4). The proton resonances at chemical shifts δ_{H} 5.07 (1 H, d, J = 7.2 Hz) and 4.66 (1 H, bs) were assigned to the anomeric protons of β -glucopyranose and α -rhamnopyranose, respectively. Additionally, the resonance observed at δ_{H} 0.94 (3 H, d, J = 6.5 Hz, H-6'''), corresponding to three protons, confirmed the presence of a rhamnose moiety. The downfield chemical shift observed at δ_{C} 66.2 ppm (C6'') in the carbon spectrum of the glucose unit indicated a possible connection of the rhamnose unit at the C6'' position. In addition, a singlet peak detected at δ_{H} 1.99 ppm implied the existence of an acetyl group, linked to the C4''' hydroxyl group of the rhamnose unit, as indicated by the downfield shifts of the H4''' at δ_{H} 4.75 (1 H, t, J = 9.3 Hz) and C4''' (74.3) resonances of rhamnose. This compound was named salvinarin (scutellarein 4'-O-methyl-7-O-rutinoside-4'''-acetate). The key HMBC correlations of compound 2 are shown in Fig. 3.

Pectolarin (Scutellarein 6, 4'-di-OCH₃ 7-O-rutinoside) (3)

White-yellowish amorphous powder; MW = 622.58. ¹H NMR (DMSO-*d*₆): 12.98 (1H, s, 5-OH), 8.06 (2 H, d, *J* = 9.2 Hz, H-2' and H-6'), 7.19 (2 H, d, *J* = 9.2 Hz, H-3' and H-5'), 6.96 (2 H, bs, H-3 and H-8), 5.15 (1H, d, *J* = 7.0 Hz, Anomeric H-1'), 4.58 (1H, bs, Anomeric H-1'''), 3.88 (3 H, s, 4'-OMe), 3.79 (3 H, s, 6-OMe), 3.18–3.68 (4 H, m, H-2''' to H-5''' of α-rhamnopyranose), 3.12–3.66 (6 H, m, H-2'' to H-6'' of β-glucopyranose), 1.09 (3 H, d, *J* = 6.5 Hz, H-6'''). ¹³C NMR (DMSO-*d*₆, based on DEPT 135, HSQC, and HMBC experiments): 182.8 (C4), 164.5 (C2), 162.9 (C4'), 157.0 (C7), 153.0 (C9), 152.6 (C5), 133.1 (C6), 128.9 (C2' and C6'), 123.1 (C1'), 115.2 (C3' and C5'), 106.4 (C10), 103.8 (C3), 100.8 (C1'', and C1'''), 94.8 (C8), 76.9 (C3''), 76.2 (C5''), 73.6 (C2''), 72.5 (C4'''), 71.2 (C3'''), 70.9 (C2'''), 70.0 (C4''), 68.8 (C5'''), 66.4 (C6''), 60.8 (6-OMe), 56.0 (4'-OMe), 18.2 (C6''').

Scutellarein 4'-O-methyl-7-O-rutinoside (4)

White-yellowish amorphous powder; MW = 608.55. ¹H NMR (DMSO-*d*₆): 12.98 (1H, s, 5-OH), 8.05 (2 H, d, *J* = 8.8 Hz, H-2' and H-6'), 7.20 (2 H, d, *J* = 8.8 Hz, H-3' and H-5'), 6.93 (2 H, bs, H-3 and H-8), 5.03 (1H, d, *J* = 7.3 Hz, Anomeric H-1'), 4.61 (1H, bs, Anomeric H-1'''), 3.88 (3 H, s, 4'-OMe), 3.18–3.68 (4 H, m, H-2''' to H-5''' of α-rhamnopyranose), 3.14–3.66 (6 H, m, H-2'' to H-6'' of β-glucopyranose), 1.12 (3 H, d, *J* = 6.5 Hz, H-6'''). ¹³C NMR (DMSO-*d*₆, based on DEPT 135, HSQC, and HMBC experiments): 182.9 (C4), 164.4 (C2), 162.8 (C4'), 151.8 (C9), 149.6 (C7), 147.2 (C5), 131.0 (C6), 128.8 (C2'

and C6'), 123.4 (C1'), 115.3 (C3' and C5'), 106.5 (C10), 103.6 (C3), 101.5 (C1''), 101.0 (C1'''), 94.2 (C8), 76.3 (C3''), 76.0 (C5''), 73.6 (C2''), 72.6 (C4'''), 71.3 (C3'''), 70.9 (C2'''), 70.1 (C4''), 68.9 (C5'''), 66.6 (C6''), 56.0 (4'-OMe), 18.3 (C6''').

5-O-Coumaroylquinic acid (5)

Yellowish amorphous powder; MW = 338.31. ¹H NMR (DMSO-*d*₆): 7.56 (1H, d, *J* = 16.2 Hz, H-7'), 7.54 (2 H, d, *J* = 8.4 Hz, H-2' and H-6'), 6.81 (2 H, d, *J* = 8.4 Hz, H-3' and H-5'), 6.35 (1H, d, *J* = 16.2 Hz, H-8'), 5.21 (1H, m, H-5), 3.85 (1H, m, H-3), 3.58 (1H, dd, *J* = 7.4, 3.37 Hz, H-4), 1.93–2.12 (2 H, m, H-2 and H-6), 1.82–1.92 (2 H, m, H-2 and H-6). ¹³C NMR (DMSO-*d*₆, based on DEPT 135, HSQC, and HMBC experiments): 176.9 (C7), 166.6 (C9'), 160.1 (C4'), 144.5 (C7'), 130.5 (C2' and C6'), 125.7 (C1'), 116.2 (C3' and C5'), 115.6 (C8'), 73.4 (C1), 71.5 (C5), 71.4 (C4), 68.0 (C3), 39.2 (C6), 35.7 (C2).

In vitro ChE inhibitory activity

The cholinergic hypothesis represents a fundamental approach to managing AD, highlighting the significant decline in the integrity of cholinergic pathways throughout all stages of the disease [3]. With this regard, the anti-ChE activity of SAHE, SADE, obtained fractions, and isolated compounds were assessed and compared with donepezil (as the positive control) (Table 1). As seen in Table 1, SAHE exhibited a good inhibitory effect on AChE (IC₅₀ = 339.8 μg/mL, 95% CI: 294.9–384.8) compared to SADE. Thus, this extract was selected for further fractionation and isolation. Moreover, although none of the fractions showed significant ChE inhibitory activity, fractions I and IV were the more effective. In addition, as indicated in Table 1, the AChE and BChE inhibitory activity of all isolated compounds is lower than that of fractions (I–IV). However, compound 1, the major isolated compound, demonstrated greater BChE inhibitory activity than the others, and its neuroprotective effects were also evaluated.

Antioxidant activity

DPPH is a free radical that can be converted into a stable molecule by accepting a hydrogen radical or an electron. SADE and SAHE were assessed for possible antioxidant activity using DPPH radical scavenging activity compared to quercetin as the positive control (IC₅₀ = 4.08 μg/mL, 95% CI: 4.01–4.15). As presented in Table 2, SAHE exhibited greater potency (IC₅₀ = 99.1 μg/mL, 95% CI: 96.0–102.2) compared to SADE and demonstrated significant antioxidant activity.

Metal chelating ability of *S. aristata*

Metal homeostasis in the central nervous system is vital due to their roles as enzyme cofactors and critical

Table 1 Cholinesterase inhibitory activity of extracts, fractions (in 500 μg/mL), and compounds 1–5 (in 40 μg/mL)^a of *S. aristata*

Sample	AChE inhibition %	BChE inhibition %
SADE	3.66 ± 0.69	35.86 ± 1.77
SAHE	62.74 ± 3.57 (IC ₅₀ = 339.8 μg/mL, 95% CI: 294.9–384.8) ^b	15.21 ± 1.15
Fraction I	23.42 ± 0.09	5.72 ± 1.60
Fraction II	21.66 ± 0.19	0.81 ± 0.12
Fraction III	19.48 ± 0.11	1.12 ± 0.31
Fraction IV	27.77 ± 0.31	17.93 ± 2.10
Fraction V	6.49 ± 0.06	0.90 ± 0.21
Compound 1	10.91 ± 1.30	18.41 ± 2.72
Compound 2	11.93 ± 2.51	5.86 ± 0.91
Compound 3	6.55 ± 0.22	10.97 ± 0.18
Compound 4	11.54 ± 0.19	10.97 ± 0.77
Compound 5	10.03 ± 0.08	3.08 ± 0.18
Donepezil	89.11 ± 3.73 (IC ₅₀ = 0.02 μM, 95% CI: 0.01–0.03)	86.60 ± 4.81 (IC ₅₀ = 1.92 μM, 95% CI: 1.82–2.03)

^a Inhibition percent are presented as mean ± SD (three independent experiments)

^b The IC₅₀ value was calculated for the sample exhibiting inhibitory activity exceeding 50%

Table 2 Free radical scavenging activity of the extracts of *S. aristata*^a

Extract	IC ₅₀ μ g/mL (95% CI)
SAHE	99.1 (96.0-102.2)
SADE	784.5 (775.8-793.3)
Quercetin	4.08 (4.01-4.15)

^a Data were acquired from three independent experiments

components in neuronal signaling. However, excessive accumulation of metal ions can induce oxidative stress, disrupt synaptic function, and ultimately result in cognitive impairments. Therefore, the bio-metal chelation hypothesis appears to be a promising therapeutic strategy for managing AD [37]. Accordingly, the metal-chelating potential of *S. aristata* extracts for Fe²⁺, Cu²⁺, and Zn²⁺ ions was evaluated. For this purpose, UV-visible absorption spectra of the extracts were recorded within the wavelength range of 260–550 nm and compared to extracts treated with Fe²⁺, Cu²⁺, and Zn²⁺ solutions.

The SAHE exhibited two absorption peaks at 326 and 277 nm. The interaction between the extract and Cu²⁺ ions led to two red shifts, from 326 nm to 332 nm and from 277 nm to 289 nm, respectively. Additionally, interactions with Fe²⁺ and Zn²⁺ resulted in a red shift from 277 nm to 281 nm and a blue shift from 326 nm to 325 nm (Fig. 4; Table 3).

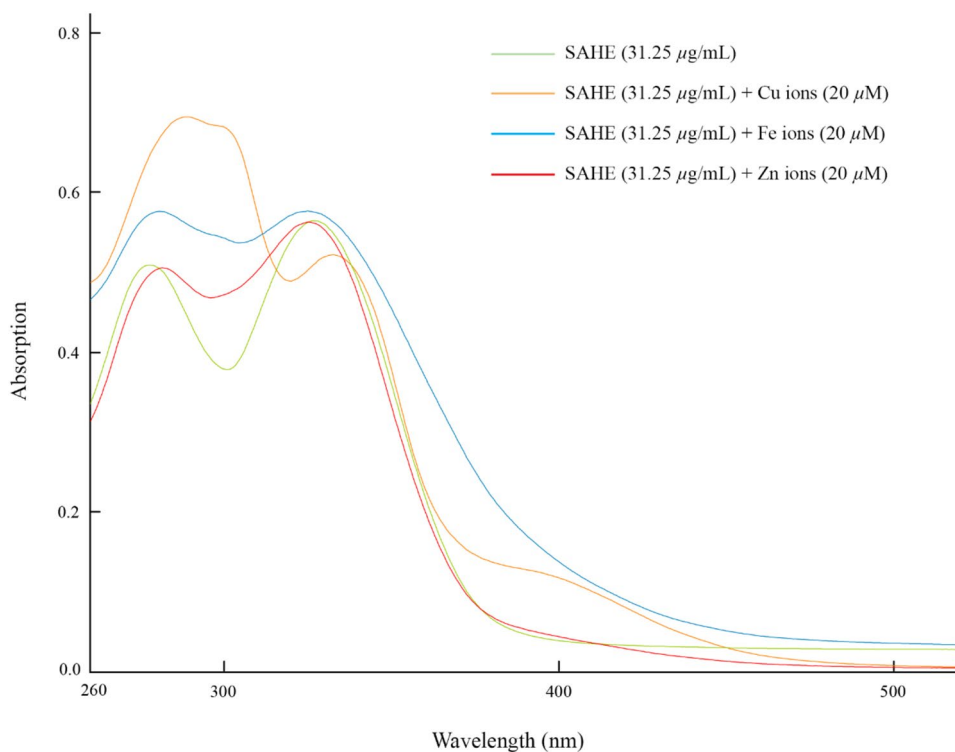
Table 3 Maximum absorption wavelength of *S. aristata* hydroalcoholic extract (SAHE) alone and in the presence of various metal ions (nm)

SAHE in MeOH	SAHE + Fe ²⁺	SAHE + Cu ²⁺	SAHE + Zn ²⁺
277	281	289	281
326	325	332	325

The UV spectrum of SADE revealed multiple absorption peaks at 532, 469, 405, 327, and 273 nm. Interaction of the extract with Cu²⁺ ions resulted in significant shifts of absorption peaks (a blue shift from 405 nm to 398 nm and a red shift from 327 nm to 333 nm). After the interaction of the sample with Fe²⁺ ions, slight blue shifts from 327 nm to 325 nm and from 273 nm to 269 nm were confirmed. In addition, when the extract was treated with Zn²⁺, only a red shift from 273 nm to 276 nm was detected (Fig. 5; Table 4).

Neuroprotectivity effects of *S. aristata* against H₂O₂-induced apoptosis in PC12 cells

The cytotoxicity of SAHE, and SADE in 2.5–20 μ g/mL and linaliin in 12.5–100 μ M were measured in comparison to the control group for PC12 cells by the AlamarBlue test. As shown in Fig. 6a-c, none of the tested concentrations exhibited any cytotoxicity after 24 h of treatment.

**Fig. 4** The absorbance changes of *S. aristata* hydroalcoholic extract (SAHE) alone (green line) and in the presence of Cu²⁺ (orange line), Fe²⁺ (blue line), and Zn²⁺ (red line) ions

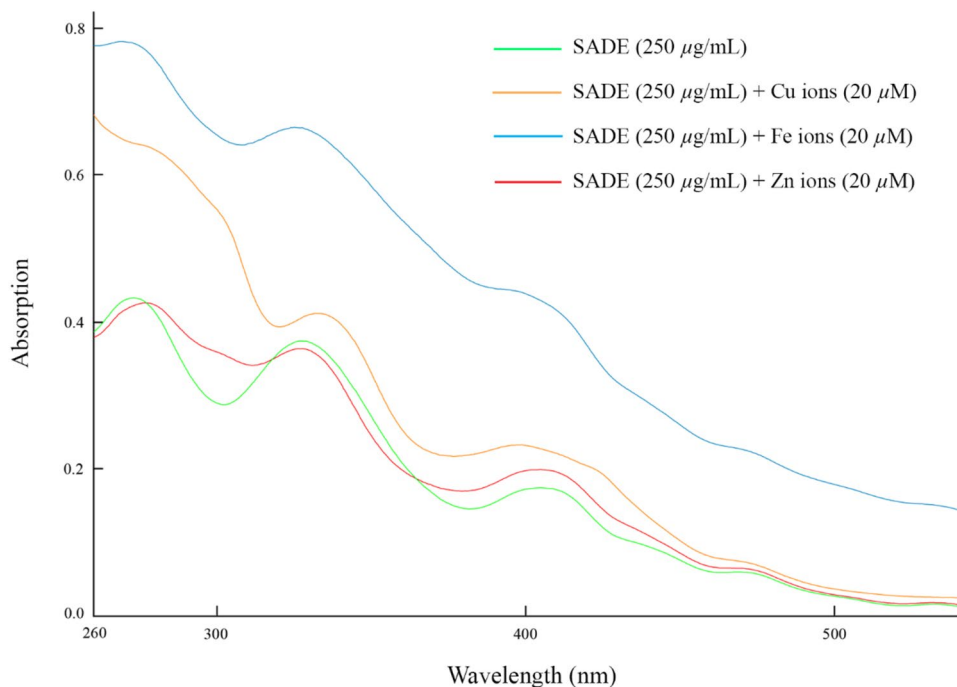


Fig. 5 The absorbance changes of *S. aristata* dichloromethane extract (SADE) alone (green line) and in the presence of Cu^{2+} (orange line), Fe^{2+} (blue line), and Zn^{2+} (red line) ions

Table 4 Maximum absorption wavelength of *S. aristata* dichloromethane extract (SADE) alone and in the presence of various metal ions (nm)

SADE in MeOH	SADE + Fe^{2+}	SADE + Cu^{2+}	SADE + Zn^{2+}
273	269	-	276
327	325	333	327
405	-	398	405

Treating PC12 cells with H_2O_2 (500 μM) could notably decrease cell viability compared to the control group ($p < 0.001$). However, pretreatment with SAHE, SADE, and linaliin notably enhanced cell viability, demonstrating strong neuroprotective effects against H_2O_2 -induced neurotoxicity (Fig. 6a'-c'). As a case in point, when PC12 cells were exposed to H_2O_2 -induced oxidative damage, cell viability rates of 90.94%, 97.67%, and 90.35% were respectively demonstrated in response to the pretreatment with 10 $\mu\text{g}/\text{mL}$ of SAHE, SADE, and 50 μM of linaliin. Furthermore, the protective effects of SAHE against H_2O_2 -induced toxicity in PC12 cells could potentially be linked to its major polyphenolic compounds, especially linaliin, which exhibited nearly 99.0% protective effect at a concentration of 100 μM (Fig. 6c'). Also, it should be noted that the NAC (5 mM) was used as the positive control ($p < 0.001$).

Effects of *S. aristata* hydroalcoholic extract on memory improvement in scopolamine-induced memory deficit rats

Knowing that memory loss is regarded as a pathognomonic symptom of AD, we performed the MWM test to assess spatial memory and learning in a rat model [38]. Scopolamine, a muscarinic cholinergic antagonist, was utilized to induce memory deficits. It can cause various cellular alterations, such as mitochondrial dysfunction, heightened oxidative stress, disruption of the antioxidant defense system, and neuroinflammation. The pathological changes induced by scopolamine resemble those found in AD patients and models, making it a valuable pharmacological tool for inducing memory deficits like AD pathogenesis [39].

Based on the in vitro anti-AChE studies, SAHE was selected for in vivo studies. The MWM test was carried out on seven groups, with each group assigned to a different treatment regimen. The experimental groups included a group that received 5 mL/kg/day of normal saline, a scopolamine group that received 4 mg/kg/day of scopolamine, a vehicle group that was given 5% ethanol in distilled water, three groups treated with different doses of SAHE (200, 300, and 400 mg/kg/day) and 4 mg/kg/day of scopolamine, and a donepezil group (positive control) that received 2.5 mg/kg/day of donepezil and 4 mg/kg/day of scopolamine. As shown in Fig. 7, the evaluation included traveled distance, escape latency, and swimming speed over the initial four days of training, as well as the time spent in the target quadrant on the fifth day during

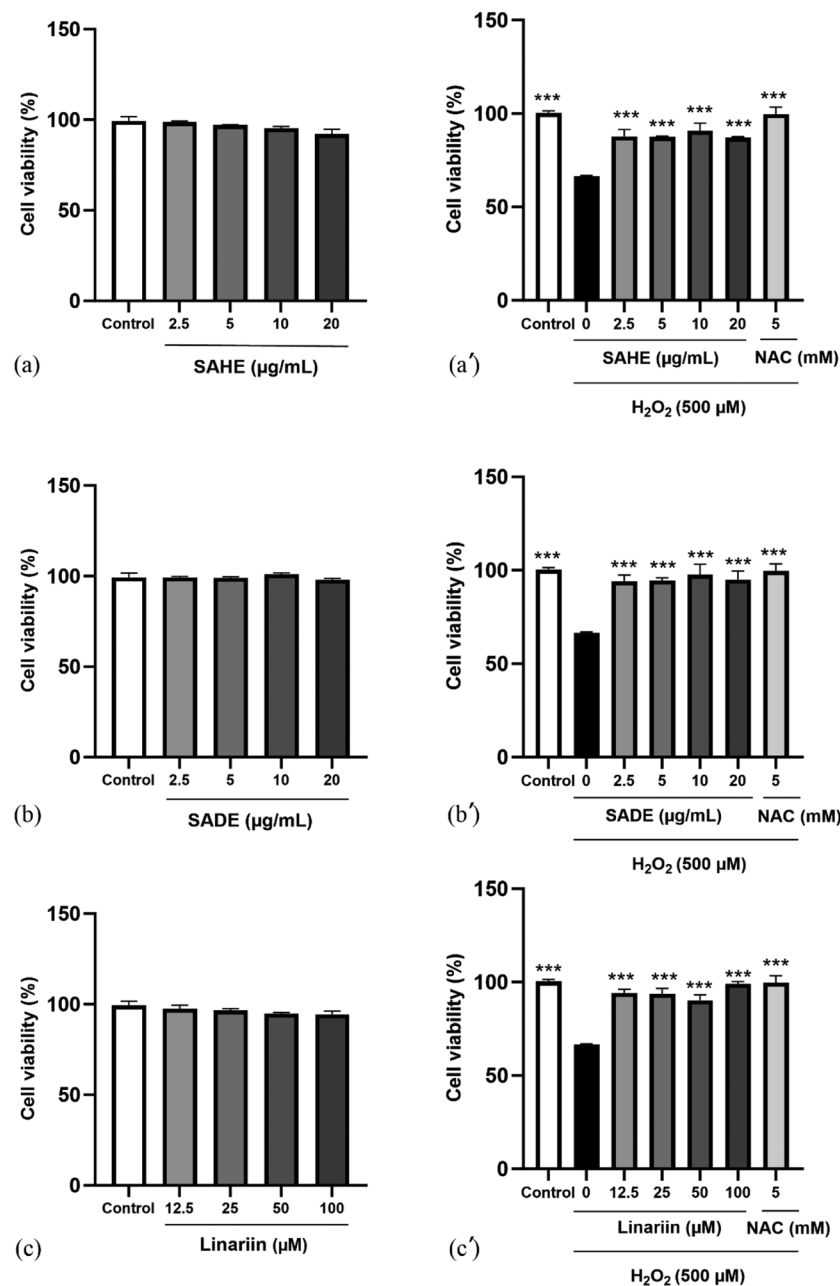


Fig. 6 Effects of various concentrations of SAHE (**a**), SADE (**b**), and linairin (**c**) on cell viability of PC12 cells after 24 h in comparison to the control group. Effects of pretreatment with various concentrations of SAHE (**a'**), SADE (**b'**), and linairin (**c'**) on H_2O_2 -induced cytotoxicity in PC12 cells. All experiments were done in triplicate. The data is presented as the mean \pm SEM. The significance of the difference is presented as * $p < 0.05$, ** $p < 0.01$, *** $p < 0.001$

the post-training probe trial. Our analysis revealed that there were no significant differences ($p > 0.05$) between the vehicle group and the control group in any of these assessments. On the other hand, scopolamine injection resulted in a significant increase in both the traveled distance ($p < 0.001$) and the escape latency ($p < 0.01$) when compared to the control group.

As shown in Fig. 7a, the groups treated with 300 and 400 mg/kg/day of SAHE in combination with scopolamine exhibited a significant improvement in the traveled

distance ($p < 0.01$ and $p < 0.001$, respectively) compared to the scopolamine group. Furthermore, administration of 300 and 400 mg/kg/day of SAHE along with scopolamine resulted in a significant decrease in the average escape latency period ($p < 0.05$ and $p < 0.001$, respectively) compared to the scopolamine-treated group (Fig. 7b). However, treatment with 200 mg/kg/day of SAHE in combination with scopolamine resulted in no significant reduction in either the mean traveled distance or the mean escape latency time. No statistically significant

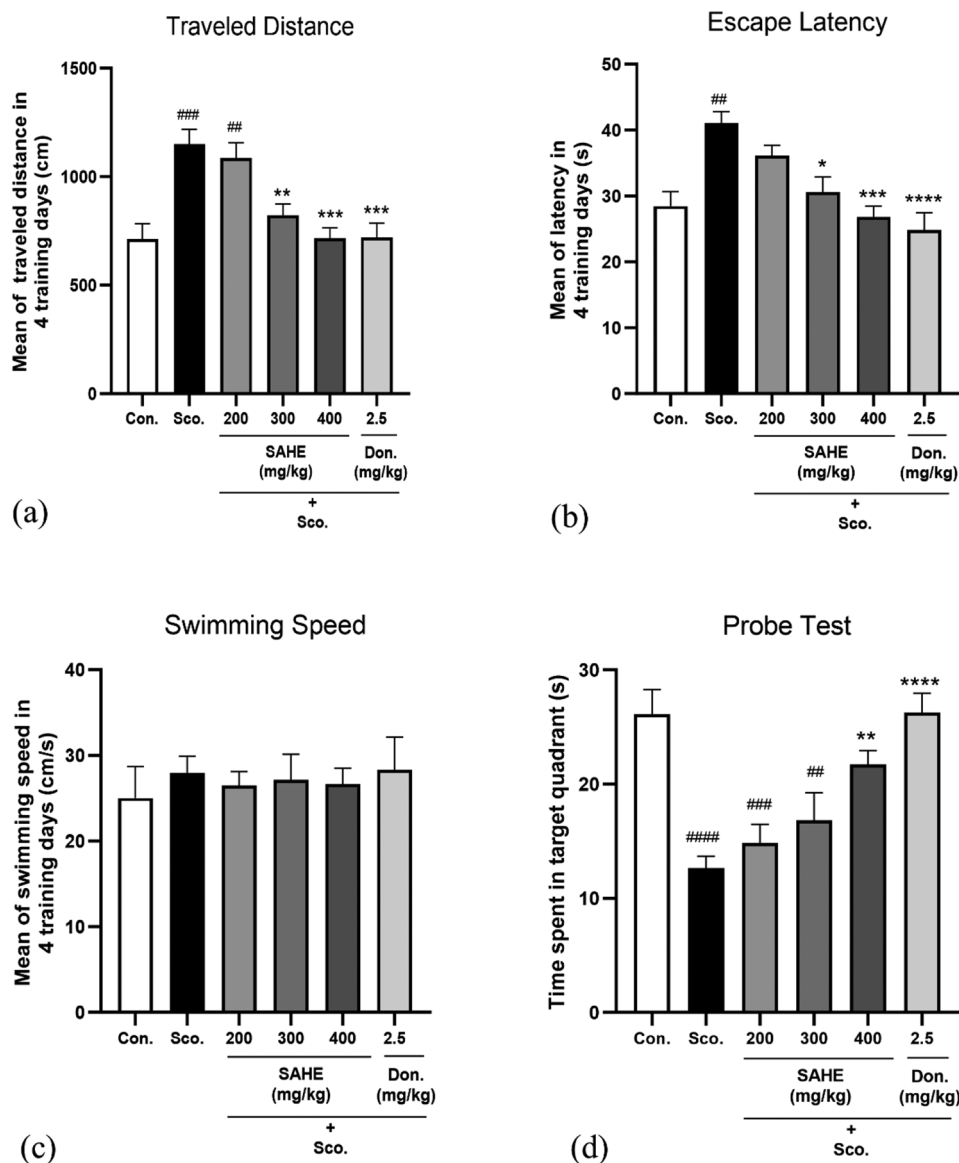


Fig. 7 The in vivo study; effects of different doses of SAHE, scopolamine, and positive control (donepezil) on the traveled distance **(a)**, escape latency **(b)**, swimming speed **(c)**, and time spent in target quadrant in probe day **(d)**. Each column displays the mean \pm SEM for seven rats. *Abbreviations:* Con., Control; Don., Donepezil; Sco., Scopolamine. * Significantly different from scopolamine groups (* $p < 0.05$, ** $p < 0.01$, *** $p < 0.001$, **** $p < 0.0001$). # Significantly different from control group (# $p < 0.05$, ## $p < 0.01$, ### $p < 0.001$, #### $p < 0.0001$)

differences in swimming speed were observed among the various treatment groups (Fig. 7c).

The post-training probe trial test was carried out on the fifth day following the training period. The trained animals were placed in the water for 90 s in the absence of the platform. To evaluate memory, the duration spent in the target quadrant (Q1) was recorded. As illustrated in Fig. 7d, the group treated with 400 mg/kg/day of SAHE alongside scopolamine exhibited a significant increase in the time spent in the target quadrant compared to the scopolamine group ($p < 0.01$). Furthermore, the positive control group receiving donepezil demonstrated a

significant improvement in memory performance relative to the scopolamine-treated group.

Discussion

In this study, we showed how extracts and linalin, the major compound of *S. aristata*, function within different pathological pathways associated with memory and AD. The results demonstrate their notable anticholinergic, antioxidant, metal-chelating, and neuroprotective properties. In particular, SAHE exhibited significantly greater bioactivity than SADE, including stronger AChE inhibition (62.74% vs. 3.66%), enhanced antioxidant capacity ($IC_{50} = 99.1 \mu\text{g/mL}$ vs. $784.5 \mu\text{g/mL}$), and superior

metal-chelating activity, as indicated by a more pronounced red shift for Cu^{2+} and Zn^{2+} (Tables 3 and 4). Due to these superior biological attributes, further phytochemical investigations were conducted on SAHE. Furthermore, this extract significantly enhanced cognitive performance in a scopolamine-induced memory impairment rat model, reinforcing its potential as a promising candidate for memory improvement.

Considering the multifactorial nature of AD, therapeutic agents derived from natural sources that target diverse pathological mechanisms stand as the preferred pharmaceutical option [40]. The *Salvia* genus has a long history of usage in AD treatment and has received increased interest in recent decades for its efficacy in neurodegenerative disorders. In this respect, many published studies have indicated the effectiveness of various species of this genus and their natural compounds in managing AD. For instance, Sezer Şenol et al. assessed 55 Turkish *Salvia* spp. for their AChE inhibitory activity and found that at a concentration of 100 $\mu\text{g}/\text{mL}$, the dichloromethane and ethyl acetate extracts of *S. fruticosa* inhibited AChE by 51.07% and 34.27%, respectively [16]. In another research, isolated compounds from the roots of *Salvia syriaca* L. showed significant AChE inhibitory activity, with IC_{50} values ranging from 24.1 to 63.0 $\mu\text{g}/\text{mL}$, comparable to galanthamine, which was used as a reference drug ($\text{IC}_{50} = 8.7 \mu\text{g}/\text{mL}$) [41].

To the best of our knowledge, this study is the first report on the ChE inhibitory activity of *S. aristata*. Our findings suggest that SAHE demonstrates significant inhibitory effects on AChE, which are consistent with previous studies [16, 41]. It is proposed that the ChE inhibitory, and neuroprotective activity of flavonoids, such as linariin is influenced by the presence of a 4'-methoxy group and the monoacetylation of the sugar moiety in their structure [42]. Additionally, in our study, salvinarin and scutellarein 4'-O-methyl-7-O-rutinoside exhibited the most potent AChE inhibitory effects among the identified flavonoids, both of which contain a hydroxyl group at the C6 position of the flavonoid backbone's A ring. These findings suggest that substituting a 6-methoxy group with a 6-hydroxy group may enhance AChE inhibitory activity. Conversely, when the sugar moiety of a flavonoid undergoes acetylation, the presence of a 6-methoxy group (as in linariin) appears to confer stronger BChE inhibitory activity than a 6-hydroxy group (as in salvinarin). Furthermore, in the absence of an acetyl group on the sugar moiety, the presence or absence of a 6-methoxy group does not seem to have a significant impact on BChE inhibition. Notably, the anti-ChE activity of SAHE in our study was greater than that of the individual isolated compounds, suggesting potential synergistic interactions among these constituents. These findings indicate that the combined effects of the isolated

compounds may contribute to ChE inhibition, potentially playing a role in AD management and memory enhancement through multiple mechanisms.

The brain, as a highly oxygen-demanding organ, is particularly prone to the creation of ROS, which can prompt the aggregation of $\text{A}\beta$, the breakdown of lysosomal membranes, and ultimately contribute to neuronal death [43, 44]. Therefore, the consumption of nutrients, such as vitamin E, and glutathione, as well as plant-derived antioxidants such as piperine can slow the progression of AD [43, 45]. In this context, the antioxidant potential of SAHE and SADE was evaluated using the DPPH radical scavenging assay, with quercetin serving as the positive control. As seen in Table 2, SAHE exhibited notable antioxidant activity, aligning with previous findings on other *Salvia* spp [46, 47]. The presence of polyhydroxy compounds in SAHE may be responsible for this effect. It has been revealed that the main mechanisms by which flavonoids demonstrate antioxidant properties include transferring hydrogen atoms to free radicals, binding with trace metal ions like Fe^{2+} and Cu^{2+} , and inhibiting prooxidant enzymes [48].

Another factor that can promote $\text{A}\beta$ deposition and oxidative stress in the brain is an imbalance in metal ions such as copper, iron, and zinc [49]. Post-mortem analyses revealed that within the amygdala of individuals diagnosed with AD, the levels of iron, copper, and zinc are 2.8, 5.7, and 3.1 times higher, respectively, compared to those in individuals without the condition [50]. Iron has a strong affinity for binding to $\text{A}\beta$, which may accelerate its oligomerization and aggregation [51]. Additionally, evidence indicates that Fe^{2+} plays a role in tau protein phosphorylation through activating the CDK5 and GSK-3 β pathways [52]. Therefore, the use of iron chelators may be considered a complementary approach in the AD treatment. In support of this, an animal study revealed that the administration of iron chelators, such as deferrioxamine, mitigated iron-induced tau protein phosphorylation in transgenic AD mice [53]. Additionally, research suggests that high concentrations of zinc ions can rapidly disrupt the stability of the $\text{A}\beta$ solution, promoting fibril formation [54]. A harmful cycle is established between oxidative stress, excessive zinc, and tau hyperphosphorylation. Increased zinc levels stimulate the production of ROS within mitochondria, while oxidative stress elevates zinc concentrations and induces tau hyperphosphorylation. Additionally, both hyperphosphorylated tau and elevated zinc contribute to neurotoxicity and oxidative damage. The disruption of microtubule function caused by hyperphosphorylated tau further amplifies oxidative stress, thus perpetuating this detrimental feedback loop [55]. Moreover, copper can form linkages with $\text{A}\beta$, generating small oligomers capable of infiltrating neurons, leading to oxidative stress and damage to them.

Furthermore, these processes may lead to a deficiency of copper in other brain areas crucial for normal functioning [56]. Hence, metal chelating agents regulate metal ion balance and represent another potential target for addressing AD. The results of metal chelating ability indicated that both SAHE and SADE can form complexes with bio-metals (Fe^{2+} , Cu^{2+} , and Zn^{2+}). However, the most significant shift in absorption peaks was observed when SAHE was exposed to Cu^{2+} ions. Furthermore, SAHE exhibited moderate activity in the presence of Zn^{2+} ions. Previous studies have shown that copper and zinc influence $\text{A}\beta$ production through different mechanisms that affect the processing of amyloid precursor protein (APP). Additionally, the modulation of APP processing and tau phosphorylation is connected to the activation of synaptic NMDA receptors induced by zinc [56]. Therefore, it is clear that the chelation of copper and zinc ions represents a promising therapeutic strategy. In addition, it should be noted that Cu^{2+} homeostasis may serve as a key regulatory point in metal ion balance, and our findings demonstrate that SAHE shows more significant chelation with Cu^{2+} than with other metal ions.

As previously mentioned, an elevation in ROS levels can result in cellular damage and cognitive impairment by affecting mitochondrial function, disrupting the balance of metal ions, and interfering with synaptic activity and neurotransmission in neurons [44, 49]. Recent findings suggest that oxidative stress serves as an early trigger for $\text{A}\beta$ plaque formation, tau protein dimerization, and subsequent hyperphosphorylation, thereby exacerbating neurodegenerative processes [57]. Consequently, targeting ROS inhibition may serve as a promising neuroprotective strategy in the pathogenesis of AD. In this study, H_2O_2 was utilized to induce cellular toxicity and oxidative damage in PC12 cells, as a suitable model to simulate cellular damages in AD. The results demonstrated that SAHE, SADE, and linaliin exhibited no cytotoxic effects relative to the control group (Fig. 3a-c). In addition, pretreatment with SAHE, SADE, and linaliin effectively reduced oxidative stress in PC12 cells and improved cell viability compared to the group treated solely with H_2O_2 (Fig. 3a'-c'). These results are consistent with previous studies that have explored the neuroprotective effects of *Salvia* spp. Tusi and Khodaghli's study [58] demonstrated that *Salvia macilenta* Boiss. possesses antiglycation properties and exerts protective effects against H_2O_2 -induced toxicity in PC12 cells. They reported a notable reduction in the Bax/Bcl-2 ratio, accompanied by decreased activation of caspase-3 and cleaved PARP. Moreover, an isolated flavonoid in our study, pectolinarin, has exhibited neuroprotective properties against H_2O_2 -induced oxidative stress in SH-SY5Y neuronal cells by reducing the release of LDH and the production of ROS [59]. Therefore, *S. aristata*, which is rich in phenolic

compounds such as linaliin, may be considered a potential neuroprotective agent.

The MWM test is widely employed to assess learning and memory, with its performance dependent on proper hippocampal function [60]. In this assessment, the spatial memory of rodents was evaluated by measuring their ability to find a hidden platform within a circular water pool [61]. In the MWM experiment, SAHE significantly reduced escape latency and traveled distance without affecting swimming speed. Furthermore, SAHE demonstrated a substantial protective effect against scopolamine-induced memory impairment in the probe test. Our findings were consistent with previous research indicating the memory-enhancing properties of other *Salvia* species [21, 62], suggesting that the administration of SAHE could effectively lead to memory improvement during scopolamine-induced impairment in an animal model of AD [31].

The memory-enhancing effects of SAHE observed in the MWM experiment may be associated with its ChE inhibitory properties and antioxidant activity. Previous studies have demonstrated that scopolamine administration leads to neurodegeneration in the prefrontal cortex of rats, along with necrotic pyramidal neurons in the CA1 and CA3 regions of the hippocampus. Additionally, scopolamine has been shown to elevate AChE activity in the cortex and hippocampus [21, 63]. Conversely, research has indicated that treatment with *Salvia* species, such as *S. officinalis* and *S. microphylla* effectively mitigates these pathological changes and restores AChE activity to normal levels [21]. Based on this evidence and our in vitro ChE inhibition results, SAHE may exert its improvement effects by suppressing ChE activity and enhancing cholinergic function, potentially through interactions with muscarinic receptors, as observed in other *Salvia* species [64]. Additional mechanisms may involve the upregulation of choline acetyltransferase activity and the enhancement of vesicular acetylcholine transporter function [65].

Furthermore, scopolamine has been shown to induce oxidative stress by decreasing glutathione levels and catalase activity while enhancing lipid peroxidation [66]. Previous studies have demonstrated that these oxidative imbalances can be reversed with *Salvia* extracts [67, 68]. In our investigation, SAHE exhibited significant in vitro antioxidant activity, suggesting that its neuroprotective effects in scopolamine-induced memory impairment may be mediated through its ability to neutralize free radicals. This effect is likely attributed to the extract's high content of polyphenolic compounds, which have been widely recognized for their antioxidant potential [69].

Finally, it can be highlighted that the polyphenolic compounds of *S. aristata* likely play a pivotal role in its diverse effects on memory improvement. Singh et al. reported that trimethoxy flavones from *Ocimum basilicum* L.

contribute to cognitive improvement by inhibiting AChE activity, reducing inflammatory markers, and enhancing antioxidant capacity through increased glutathione levels [69]. In addition, previous studies have underscored the significance of polyphenols in mitigating neurodegeneration by reducing oxidative stress, inhibiting ChE activity, and chelating metal ions [70, 71]. Therefore, the memory-enhancing effects of SAHE may be attributed to its polyphenolic content, particularly its ability to inhibit ChE, exert antioxidant properties, and chelate metal ions.

Conclusion

In this study, a new flavonoid (salvianarin, **2**) and four known phenolic compounds (**1**, and **3–5**) were isolated from the hydroalcoholic extract of *S. aristata* for the first time. Moreover, the biological effects of this plant on memory deficits and AD were extensively investigated through both in vitro and in vivo studies. Our findings indicated that SAHE and its major compound, linariin (**1**), exhibited significant neuroprotective effects against H₂O₂-induced cytotoxicity in PC12 cells, along with ChE inhibitory activity. Additionally, the SAHE has demonstrated antioxidant and metal-chelating activities and could prevent memory deficits induced by scopolamine in a rat model by improvement in cholinergic transmission. These effects could be ascribed to the synergistic interactions among its polyphenolic compounds. Given these promising results, further research is essential to elucidate the precise molecular mechanisms underlying the neuroprotective properties of *S. aristata*, particularly in relation to polyphenol interactions with cholinergic pathways and oxidative stress. Future studies should also explore its pharmacokinetics, bioavailability, and safety profile through preclinical and clinical evaluations. Overall, *S. aristata* holds promise as a potential natural therapeutic agent for the prevention and treatment of memory deficits, warranting further multidisciplinary research in neuropharmacology and drug development.

Abbreviations

AChE	Acetylcholinesterase
AD	Alzheimer's disease
BChE	Butyrylcholinesterase
CC	Column chromatography
ChE	Cholinesterase
CI	Confidence interval
DPPH	1, 1-diphenyl-2-picrylhydrazyl
ROS	Reactive oxygen species
SADE	<i>S. aristata</i> dichloromethane extract
SAHE	<i>S. aristata</i> hydroalcoholic extract
MWM	Morris water maze
NAC	N-acetyl cysteine

Supplementary Information

The online version contains supplementary material available at <https://doi.org/10.1186/s12906-025-04902-1>.

Supplementary Material 1: ¹H-NMR, ¹³C-NMR, DEPT 135, HSQC, and HMBC spectra of compounds **1–5**, as well as HRESI-MS, UV, and IR spectra of compound **2** are available as Supporting Information.

Acknowledgements

We thank the Deputy of Research and Technology at Tehran University of Medical Sciences (Tehran, Iran).

Author contributions

FD performed the chemical parts, structure elucidation, biological experiments (antioxidant and metal chelating activity), and prepared the original draft. MRD contributed to the conception, experimental design of chemical parts, and structural elucidation. RH completed biological experiments (cholinesterase inhibitory activity). TA supervised biological experiments (cholinesterase inhibitory activity). ZT contributed to the conception and experimental design of the biological parts (neuroprotectivity assay). MRSA contributed to the conceptualization. MS supervised pharmacological parts. MK was responsible for the study conception, design, and supervision of all parts of the study. All authors reviewed and approved the final manuscript.

Funding

This work was supported by grants from the Research Council of Tehran University of Medical Sciences with project No. 98-3-104-45596.

Data availability

All data generated or analysed during this study are included in this published article and its supplementary information files.

Declarations

Ethics approval and consent to participate

Experimental research and field studies on plants, including the collection of plant material, comply with relevant institutional, national, and international guidelines and legislation. Animal treatment and maintenance were carried out in strict compliance with the "Institutional Guide for the Care and Use of Laboratory Animals" guidelines and were approved by the Tehran University of Medical Sciences Ethical Committee for the Care and Use of Laboratory Animals (approval ID: IRTUMS.TIPS.REC.1398.153 at January 4th 2020).

Consent for publication

Not applicable.

Competing interests

The authors declare no competing interests.

Author details

¹Department of Pharmacognosy, Faculty of Pharmacy, and Persian Medicine and Pharmacy Research Center, Tehran University of Medical Sciences, Tehran, Iran

²Department of Medicinal Chemistry, Faculty of Pharmacy, Tehran University of Medical Sciences, Tehran, Iran

³Targeted Drug Delivery Research Center, Pharmaceutical Technology Institute, Mashhad University of Medical Sciences, Mashhad, Iran

⁴Department of Pharmacology and Toxicology, Faculty of Pharmacy, Tehran University of Medical Sciences, Tehran, Iran

Received: 22 September 2024 / Accepted: 28 April 2025

Published online: 17 May 2025

References

- Scheltens P, De Strooper B, Kivipelto M, Holstege H, Chételet G, Teunissen CE, et al. Alzheimer's disease. *Lancet*. 2021;397(10284):1577–90.
- Guo T, Zhang D, Zeng Y, Huang TY, Xu H, Zhao Y. Molecular and cellular mechanisms underlying the pathogenesis of Alzheimer's disease. *Mol Neurodegener*. 2020;15(1):1–37.

3. Nemy M, Dyrba M, Brosseron F, Buerger K, Dechent P, Dobisch L, et al. Cholinergic white matter pathways along the Alzheimer's disease continuum. *Brain*. 2023;146(5):2075–88.
4. Shin J, Kong C, Lee J, Choi BY, Sim J, Koh CS, et al. Focused ultrasound-induced blood-brain barrier opening improves adult hippocampal neurogenesis and cognitive function in a cholinergic degeneration dementia rat model. *Alzheimers Res Ther*. 2019;11:1–15.
5. Afsar A, Chacon Castro MC, Soladogun AS, Zhang L. Recent development in the Understanding of molecular and cellular mechanisms underlying the etiopathogenesis of Alzheimer's disease. *Int J Mol Sci*. 2023;24(8):7258.
6. Dabaghian F, Hasanpour M, Maroufizadeh S, Joulani MH. Use of medicinal plants and its association with health literacy in the general population of Iran during the COVID-19 pandemic: a Web-Based Cross-Sectional survey. *Res J Pharmacogn*. 2023;10(1):31–40.
7. Liu J, Li T, Zhong G, Pan Y, Gao M, Su S, et al. Exploring the therapeutic potential of natural compounds for Alzheimer's disease: mechanisms of action and Pharmacological properties. *Biomed Pharmacother*. 2023;166:115406.
8. Umukoro S, Okoh L, Igweze SC, Ajayi AM, Ben-Azu B. Protective effect of *Cyperus esculentus* (tiger nut) extract against scopolamine-induced memory loss and oxidative stress in mouse brain. *Drug Metab Pers Ther*. 2020;35(3):20200112.
9. Vicente-Zurdo D, Gómez-Mejía E, Rosales-Conrado N, León-González ME. A comprehensive analytical review of polyphenols: evaluating neuroprotection in Alzheimer's disease. *Int J Mol Sci*. 2024;25(11):5906.
10. Gentile MT, Camerino I, Ciarmiello L, Woodrow P, Musciariello L, De Chiara I, et al. Neuro-nutraceutical polyphenols: how Far are we? *Antioxidants*. 2023;12(3):539.
11. Albadrani HM, Chauhan P, Ashique S, Babu MA, Iqbal D, Almutary AG, et al. Mechanistic insights into the potential role of dietary polyphenols and their nanoformulation in the management of Alzheimer's disease. *Biomed Pharmacother*. 2024;174:116376.
12. Azarogonjahreni A, Abutalebian F. Unraveling the therapeutic efficacy of Resveratrol in Alzheimer's disease: an umbrella review of systematic evidence. *Nutr Metab*. 2024;21(1):15.
13. Vijh D, Imam MA, Haque MMU, Das S, Islam A, Malik MZ. Network Pharmacology and bioinformatics approach reveals the therapeutic mechanism of action of Curcumin in alzheimer disease. *Metab Brain Dis*. 2023;38(4):1205–20.
14. Hussain H, Ahmad S, Shah SWA, Ullah A, Ali N, Almeahadi M, et al. Attenuation of scopolamine-induced amnesia via cholinergic modulation in mice by synthetic Curcumin analogs. *Molecules*. 2022;27(8):2468.
15. Howes M-JR, Houghton PJ. Traditional medicine for memory enhancement. In: Ramawat KG, editor. *Herbal drugs: ethnomedicine to modern medicine*. Berlin, Heidelberg: Springer; 2009. pp. 239–91.
16. Şenol FS, Orhan I, Celep F, Kahraman A, Doğan M, Yılmaz G, et al. Survey of 55 Turkish *Salvia* taxa for their acetylcholinesterase inhibitory and antioxidant activities. *Food Chem*. 2010;120(1):34–43.
17. Topcu G, Kolak U, Ozturk M, Boga M, Damla Hatipoglu S, Bahadori F, et al. Investigation of anticholinesterase activity of a series of *Salvia* extracts and the constituents of *Salvia staminea*. *Nat Prod J*. 2013;3(1):3–9.
18. Ververis A, Savvidou G, Ioannou K, Nicolaou P, Christodoulou K, Plioukas M. Greek Sage exhibits neuroprotective activity against amyloid beta-induced toxicity. *Evid Based Complement Alternat Med*. 2020;2020(1):2975284.
19. Mervić M, Bival Štefan M, Kindl M, Blažeković B, Marijan M, Vladimir-Knežević. Comparative antioxidant, anti-acetylcholinesterase and anti- α -glucosidase activities of mediterranean *Salvia* species. *Plants*. 2022;11(5):625.
20. Datta S, Patil S. Evaluation of traditional herb extract *Salvia officinalis* in treatment of alzheimers disease. *Pharmacogn J*. 2020;12(1).
21. Ayoub IM, George MY, Menze ET, Mahmoud M, Botros M, Essam M, et al. Insights into the neuroprotective effects of *Salvia officinalis* L. and *Salvia microphylla* Kunth in the memory impairment rat model. *Food Funct*. 2022;13(4):2253–68.
22. Zhou Y, Li W, Xu L, Chen L. *Salvia miltiorrhiza*, phenolic acids possess protective properties against amyloid β -induced cytotoxicity, and Tanshinones act as acetylcholinesterase inhibitors. *Environ Toxicol Pharmacol*. 2011;31(3):443–52.
23. Ozarowski M, Mikolajczak PL, Piasecka A, Kujawski R, Bartkowiak-Wieczorek J, Bogacz A, et al. Effect of *Salvia miltiorrhiza* root extract on brain acetylcholinesterase and butyrylcholinesterase activities, their mRNA levels and memory evaluation in rats. *Physiol Behav*. 2017;173:223–30.
24. Moein F, Jamzad Z, Rahiminejad M. An integrating study of genetic diversity and ecological niche modelling in *Salvia aristata* (Lamiaceae). *Acta Bot Hung*. 2019;61(1–2):185–204.
25. Dabaghian F, Aalinezhad S, Delnavazi MR, Saeedi M, Khanavi* M. *Salvia aristata* essential oil: chemical composition, cholinesterase Inhibition, and neuroprotective effects against oxidative stress in PC12 cells. *Res J Pharmacogn*. 2025;12(2):65–75.
26. Esmaeili M, Alilou M, Sonboli A. Neuroprotective effects of *Salvia aristata* Aucher ex Benth. On hydrogen peroxide induced apoptosis in SH-SY5Y neuroblastoma cells. *Res J Pharmacogn*. 2015;2(4):17–26.
27. Gharehbagh HJ, Ebrahimi M, Dabaghian F, Mojtabavi S, Hariri R, Saeedi M, et al. Chemical composition, cholinesterase, and α -glucosidase inhibitory activity of the essential oils of some Iranian native *Salvia* species. *BMC Complement Med Ther*. 2023;23(1):1–16.
28. Hussain H, Ahmad S, Shah SWA, Ullah A, Almeahadi M, Abdulaziz O, et al. Investigation of antistress and antidepressant activities of synthetic Curcumin analogues: behavioral and biomarker approach. *Biomedicine*. 2022;10(10):2385.
29. Rastegari A, Manayi A, Rezakazemi M, Eftekhari M, Khanavi M, Akbarzadeh T, et al. Phytochemical analysis and anticholinesterase activity of Aril of *Myristica fragrans* Houtt. *BMC Chem*. 2022;16(1):106.
30. Hadipour E, Tayarani-Najaran Z, Fereidoni M. Vitamin K2 protects PC12 cells against A β (1–42) and H₂O₂-induced apoptosis via p38 MAP kinase pathway. *Nutr Neurosci*. 2020;23(5):343–52.
31. Najafi Z, Mahdavi M, Saeedi M, Karimpour-Razkenari E, Edraki N, Sharifzadeh M, et al. Novel tacrine-coumarin hybrids linked to 1, 2, 3-triazole as anti-Alzheimer's compounds: in vitro and in vivo biological evaluation and Docking study. *Bioorg Chem*. 2019;83:303–16.
32. Kishore S, Anitha K, Nettem S, Pratima K, Shobana K. Evaluation of nootropic activity of *Salvia officinalis* L. extract using different experimental models in rats. *Global Trends Pharm Sci*. 2014;5(4):2115–7.
33. Ercil D, Sakar MK, Olmo ED, Feliciano AS. Chemical constituents of *Linaria aucheri*. *Turk J Chem*. 2004;28(1):133–40.
34. Cho S, Lee J, Lee YK, Chung MJ, Kwon KH, Lee S. Determination of Pectolarin in *Cirsium* spp. Using HPLC/UV analysis. *J Appl Biol Chem*. 2016;59(2):107–12.
35. Grayer RJ, Veitch NC, Kite GC, Paton AJ, Garnock-Jones PJ. Scutellarein 4'-methyl ether glycosides as taxonomic markers in Teucrium and Tripora (Lamiaceae, Ajugoideae). *Phytochemistry*. 2002;60(7):727–31.
36. Wan C, Yuan T, Cirello AL, Seeram NP. Antioxidant and α -glucosidase inhibitory phenolics isolated from highbush blueberry flowers. *Food Chem*. 2012;135(3):1929–37.
37. Das N, Raymick J, Sarkar S. Role of metals in Alzheimer's disease. *Metab Brain Dis*. 2021;36(7):1627–39.
38. Sanati M, Khodaghohi F, Aminyavari S, Ghasemi F, Gholami M, Kebriaeezadeh A, et al. Impact of gold nanoparticles on amyloid β -induced Alzheimer's disease in a rat animal model: involvement of STIM proteins. *ACS Chem Neurosci*. 2019;10(5):2299–309.
39. San Tang K. The cellular and molecular processes associated with scopolamine-induced memory deficit: A model of Alzheimer's biomarkers. *Life Sci*. 2019;233:116695.
40. Chen X, Drew J, Berney W, Lei W. Neuroprotective natural products for Alzheimer's disease. *Cells*. 2021;10(6):1309.
41. Bahadori MB, Dinparast L, Valizadeh H, Farimani MM, Ebrahimi SN. Bioactive constituents from roots of *Salvia syriaca* L.: acetylcholinesterase inhibitory activity and molecular Docking studies. *S Afr J Bot*. 2016;106:1–4.
42. Uriarte-Pueyo I, Calvo MI. Structure–activity relationships of acetylated flavone glycosides from *Galeopsis ladanum* L. (Lamiaceae). *Food Chem*. 2010;120(3):679–83.
43. Dwivedi D, Megha K, Mishra R, Mandal PK. Glutathione in brain: overview of its conformations, functions, biochemical characteristics, quantitation and potential therapeutic role in brain disorders. *Neurochem Res*. 2020;45:1461–80.
44. Misrani A, Tabassum S, Yang L. Mitochondrial dysfunction and oxidative stress in Alzheimer's disease. *Front Aging Neurosci*. 2021;13:57.
45. Dabaghian F, Azadi A, Zarshenas MM. Design, reformulation, and standardization of a traditional-based memory enhancer herbal Preparation originated from Persian medicine. *J Med Plants*. 2022;21(82):93–110.
46. Poulies E, Giaginis C, Vasios GK. Current state of the Art on the antioxidant activity of Sage (*Salvia* spp.) and its bioactive components. *Planta Med*. 2020;86(04):224–38.

47. Jeshvaghani ZA, Rahimmalek M, Talebi M, Goli SAH. Comparison of total phenolic content and antioxidant activity in different *Salvia* species using three model systems. *Ind Crops Prod*. 2015;77:409–14.
48. Amic D, Davidovic-Amic D, Beslo D, Rastija V, Lucic B, Trinajstic N. SAR and QSAR of the antioxidant activity of flavonoids. *Curr Med Chem*. 2007;14(7):827–45.
49. Chen L-L, Fan Y-G, Zhao L-X, Zhang Q, Wang Z-Y. The metal ion hypothesis of Alzheimer's disease and the anti-neuroinflammatory effect of metal chelators. *Bioorg Chem*. 2023;131:106301.
50. Lovell M, Robertson J, Teesdale W, Campbell J, Markesbery W. Copper, iron and zinc in Alzheimer's disease senile plaques. *J Neurol Sci*. 1998;158(1):47–52.
51. House E, Collingwood J, Khan A, Korchazkina O, Berthon G, Exley C. Aluminium, iron, zinc and copper influence the in vitro formation of amyloid fibrils of A β 42 in a manner which may have consequences for metal chelation therapy in Alzheimer's disease. *J Alzheimers Dis*. 2004;6(3):291–301.
52. Lovell MA, Xiong S, Xie C, Davies P, Markesbery WR. Induction of hyperphosphorylated Tau in primary rat cortical neuron cultures mediated by oxidative stress and glycogen synthase kinase-3. *J Alzheimers Dis*. 2004;6(6):659–71.
53. Guo C, Wang P, Zhong M-L, Wang T, Huang X-S, Li J-Y, et al. Deferoxamine inhibits iron induced hippocampal Tau phosphorylation in the Alzheimer Transgenic mouse brain. *Neurochem Int*. 2013;62(2):165–72.
54. Xie Z, Wu H, Zhao J. Multifunctional roles of zinc in Alzheimer's disease. *Neurotoxicology*. 2020;80:112–23.
55. Lai C, Chen Z, Ding Y, Chen Q, Su S, Liu H, et al. Rapamycin attenuated zinc-induced Tau phosphorylation and oxidative stress in rats: involvement of dual mTOR/p70S6K and Nrf2/HO-1 pathways. *Front Immunol*. 2022;13:782434.
56. Liu Y, Nguyen M, Robert A, Meunier B. Metal ions in Alzheimer's disease: a key role or not? *Acc Chem Res*. 2019;52(7):2026–35.
57. Roy RG, Mandal PK, Maroon JC. Oxidative stress occurs prior to amyloid A β plaque formation and Tau phosphorylation in Alzheimer's disease: role of glutathione and metal ions. *ACS Chem Neurosci*. 2023;14(17):2944–54.
58. Tusi SK, Khodaghohi F. *Salvia macilenta* exhibits antiglycating activity and protects PC12 cells against H₂O₂-induced apoptosis. *Cytotechnology*. 2014;66:169–79.
59. Pang QQ, Kim JH, Kim HY, Kim J-H, Cho EJ. Protective effects and mechanisms of Pectolarin against H₂O₂-Induced oxidative stress in SH-SY5Y neuronal cells. *Molecules*. 2023;28(15):5826.
60. Othman MZ, Hassan Z, Has ATC. Morris water maze: a versatile and pertinent tool for assessing Spatial learning and memory. *Exp Anim*. 2022;71(3):264–80.
61. Vorhees CV, Williams MT. Morris water maze: procedures for assessing Spatial and related forms of learning and memory. *Nat Protoc*. 2006;1(2):848–58.
62. Dinel A-L, Lucas C, Guillemet D, Layé S, Pallet V, Joffre C. Chronic supplementation with a mix of *Salvia officinalis* and *Salvia Lavandulaefolia* improves Morris water maze learning in normal adult C57Bl/6J mice. *Nutrients*. 2020;12(6):1777.
63. Akbarian M, Mirzavi F, Amirahmadi S, Hosseini M, Alipour M, Feizi H, et al. Amelioration of oxidative stress, cholinergic dysfunction, and neuroinflammation in scopolamine-induced amnesic rats fed with pomegranate seed. *Inflammopharmacology*. 2022;30(3):1021–35.
64. Eidi M, Eidi A, Bahar M. Effects of *Salvia officinalis* L.(sage) leaves on memory retention and its interaction with the cholinergic system in rats. *Nutrition*. 2006;22(3):321–6.
65. Sharifzadeh M, Naghdi N, Khosrovani S, Ostad SN, Sharifzadeh K, Roghani A. Post-training intrahippocampal infusion of the COX-2 inhibitor celecoxib impaired Spatial memory retention in rats. *Eur J Pharmacol*. 2005;511(2–3):159–66.
66. Haider S, Tabassum S, Perveen T. Scopolamine-induced greater alterations in neurochemical profile and increased oxidative stress demonstrated a better model of dementia: a comparative study. *Brain Res Bull*. 2016;127:234–47.
67. Lee J, Lee S, Jo W, Ji HW, Pyeon M, Moon M, et al. Effect of a *Salvia officinalis* and *Hypericum perforatum* mixture on improving memory and cognitive decline. *Adv Tradit Med*. 2024;24(2):633–49.
68. Wahid F, Jan T, Al-Joufi FA, Ali Shah SW, Nisar M, Zahoor M. Amelioration of scopolamine-induced cognitive dysfunction in experimental mice using the medicinal plant *Salvia Moorcroftiana*. *Brain Sci*. 2022;12(7):894.
69. Singh V, Kaur K, Kaur S, Shri R, Singh TG, Singh M. Trimethoxyflavones from *Ocimum basilicum* L. leaves improve long term memory in mice by modulating multiple pathways. *J Ethnopharmacol*. 2022;295:115438.
70. Lakey-Beitia J, Burillo AM, La Penna G, Hegde ML, Rao K. Polyphenols as potential metal chelation compounds against Alzheimer's disease. *J Alzheimers Dis*. 2021;82(s1):S335–57.
71. Randhawa K, Singh V, Kaur S, Kaur R, Kumar S, Shri R. Isolation of *Pleurotus florida* derived acetylcholinesterase inhibitor for the treatment of cognitive dysfunction in mice. *Food Sci Hum Wellness*. 2021;10(4):490–6.

Publisher's note

Springer Nature remains neutral with regard to jurisdictional claims in published maps and institutional affiliations.